Korean J Physiol Pharmacol 2022;26(5):335-345
https://doi.org/10.4196/kjpp.2022.26.5.335

KJPP

Original Article

Tanshinone IIA reduces pyroptosis in rats with coronary microembolization by inhibiting the TLR4/MyD88/NF-κB/NLRP3 pathway

Hao-Liang Li, Tao-Li, Zhi-Qing Chen, and Lang Li*

Department of Cardiology, The First Affiliated Hospital of Guangxi Medical University & Guangxi Key Laboratory Base of Precision Medicine in Cardio-Cerebrovascular Diseases Control and Prevention & Guangxi Clinical Research Center for Cardio-Cerebrovascular Diseases, Nanning 530021, People's Republic of China

ARTICLE INFO

Received April 6, 2022
Revised May 11, 2022
Accepted May 14, 2022

***Correspondence**
Lang Li
E-mail: drlilang1968@126.com

Key Words
Coronary microembolization
Pyroptosis
Tanshinone IIA
TLR4/MyD88/NF-κB/NLRP3 cascade

ABSTRACT Pyroptosis is an inflammatory form of programmed cell death that is linked with invading intracellular pathogens. Cardiac pyroptosis has a significant role in coronary microembolization (CME), thus causing myocardial injury. Tanshinone IIA (Tan IIA) has powerful cardioprotective effects. Hence, this study aimed to identify the effect of Tan IIA on CME and its underlying mechanism. Forty Sprague–Dawley (SD) rats were randomly grouped into sham, CME, CME + low-dose Tan IIA, and CME + high-dose Tan IIA groups. Except for the sham group, polyethylene microspheres (42 μm) were injected to establish the CME model. The Tan-L and Tan-H groups received intraperitoneal Tan IIA for 7 days before CME. After CME, cardiac function, myocardial histopathology, and serum myocardial injury markers were assessed. The expression of pyroptosis-associated molecules and TLR4/MyD88/NF-κB/NLRP3 cascade was evaluated by qRT-PCR, Western blotting, ELISA, and IHC. Relative to the sham group, CME group's cardiac functions were significantly reduced, with a high level of serum myocardial injury markers, and microinfarct area. Also, the levels of caspase-1 p20, GSDMD-N, IL-18, IL-1β, TLR4, MyD88, p-NF-κB p65, NLRP3, and ASC expression were increased. Relative to the CME group, the Tan-H and Tan-L groups had considerably improved cardiac functions, with a considerably low level of serum myocardial injury markers and microinfarct area. Tan IIA can reduce the levels of pyroptosis-associated mRNA and protein, which may be caused by inhibiting TLR4/MyD88/NF-κB/NLRP3 cascade. In conclusion, Tanshinone IIA can suppress cardiomyocyte pyroptosis probably through modulating the TLR4/MyD88/NF-κB/NLRP3 cascade, lowering cardiac dysfunction, and myocardial damage.

INTRODUCTION

Coronary microembolization (CME) is a distal microcirculatory embolization caused by the shedding of atherosclerotic plaque rupture in acute coronary syndrome or percutaneous coronary intervention [1,2]. CME often leads to reduction in coronary flow reserve, myocardial contraction function decline, and fatal arrhythmia. CME is thought to be a reliable predictor of severe cardiac events and poor long-term prognosis [3,4]. However, there is a lack of clarity regarding CME-induced myocardial damage. Pyroptosis is a recently found type of programmed cell death that was originally observed in Salmonella-induced macrophage mortality [5]. It has been closely associated with inflammasomes, caspase family, and gasdermin proteins. The nod-like receptor protein 3 (NLRP3) inflammasome, which includes proteins, such as NLRP3, apoptosis-associated speck-like protein contain a CARD

Author contributions: H.L.L., T.L., and Z.Q.C. conducted the experiments and data analysis. L.L. and H.L.L. participated in the design, interpretation of the study, wrote and reviewed critical revision of the article. All authors read and approved the final manuscript.

(ASC), and caspase-1 [6], was found to be linked to classical pyroptosis. Furthermore, gasdermin D (GSDMD) is the executor of pyroptotic cell death. Studies have shown that caspase-1/4/5/11 can cleave GSDMD, resulting in cellular rupture and the release of proinflammatory cytokines [7,8]. Pyroptosis contributes to the onset and progression of a number of cardiovascular diseases. Hence, inhibiting cardiomyocyte pyroptosis could be a possible CME therapy.

Toll-like receptors (TLRs) are crucial pattern recognition receptors that recognize various pathogen-associated molecule patterns (PAMP) and play an important role in natural immunity [9]. TLR4 belongs to a TLR family that mediates inflammatory responses in the myocardium. TLR4 can trigger the NF-κB inflammatory pathway through MyD88 [10]. Furthermore, TLR4/MyD88/NF-κB signaling cascade triggers NLRP3 to promote inflammatory cascade reaction and aggravate myocardial injury [11]. It has been reported that TLR4/Myd88/NF-κB cascade and NLRP3 inflammasome contributed to CME-mediated myocardial damage. TAK-242, an inhibitor of TLR4, can reduce NLRP3 inflammasome stimulation by attenuating TLR4/MyD88/NF-κB cascade, thus inhibiting the myocardial inflammatory response and alleviating myocardial injury after CME [12]. Hence, we proposed that attenuation of TLR4/MyD88/NF-κB/NLRP3 cascade can significantly block cardiomyocyte pyroptosis and enhance cardiac function post CME.

Tanshinone IIA (Tan IIA) is a fat-soluble compound obtained from the traditional Chinese medicine Salvia miltiorrhiza Bunge, named Danshen. It has anti-inflammatory, anti-oxidation, and anti-apoptotic impact, and has been widely used as an effective drug against cardiovascular diseases because of its cardioprotective effects [13,14]. At present, whether Tanshinone IIA can alleviate CME-induced myocardial injury is still undemonstrated. Hence, we aimed to identify the influence of Tanshinone IIA on CME and its molecular mechanism.

METHODS

Animal preparation and grouping

The approval for experimental studies was obtained from Guangxi Medical University's Animal Ethics Committee, and each experiment was carried out in accordance with the National Institute of Health Guidelines on the Use of Laboratory Animals. Forty healthy Sprague–Dawley rats (male, 250–300 g) were procured from the Medical Experimental Animal Center of Guangxi Medical University. The rats were kept in a place with the following conditions: water and food: free access; light/dark period: 12 h/12 h; temp: 23 ± 2°C; humidity: 50%–60%. Randomly, four groups (10 rats per group) of these animals were formed: the sham, the CME, the CME + low-dose Tan IIA (10 mg/kg, Tan-L), and the CME + high-dose Tan IIA (20 mg/kg, Tan-H) group. Different dosages of Tanshinone IIA (Shanghai yuanye Bio-Technology Co., Ltd., Shanghai, China) were intraperitoneally administered for one week before initiating CME, as reported previously [15].

Establishment of CME model

As previously described [16], a rat CME model was developed. The rats were anaesthetized with pentobarbital sodium (30–40 mg/kg) administered intraperitoneally. To aid breathing, a small ventilator, specially designed for animals, was connected to rats. The ascending aorta was separated, followed by clamping for 10 sec using a vascular clamp after a left lateral thoracotomy was completed *via* the 3rd and 4th intercostal gaps. In addition, 3,000 polyethylene microspheres with a diameter of 42 μm (Biosphere Medical Inc., Rockland, MA, USA) were suspended in 0.1 ml of normal saline, followed by rapidly introducing into the left ventricle with microinjector. The sham group was treated with only 0.1 ml of normal saline. The chest skin was sutured until the rat's heart beat returned to normal, and the tracheal tube was detached from the ventilator until normal breathing returned. To avoid infections, the rats were given penicillin (800,000 units) intraperitoneally.

Cardiac function assessment

Reported studies have shown that the cardiac function is worst at 12 h after CME [17]. Hence, we chose to evaluate rat heart function at this point. A Hewlett Packard Sonos 7500 ultrasound machine (Philips Technologies, Amsterdam, NY, USA) with a transducer (12 MHz) was employed to calculate the left ventricular end-systolic diameter, left ventricular end-diastolic diameter, left ventricular fractional shortening, and left ventricular ejection fraction, abbreviated as LVESd, LVEDd, LVFS, and LVEF accordingly. The average of three cardiac cycles was used for all measurements. The echocardiography was conducted by an experienced individual.

Determination of serum myocardial injury markers and inflammatory factors

From the femoral vein of each rat, 2 ml of blood was taken 12 h after the sham or CME operation. Following the manufacturer's provided guidelines, enzyme-linked immunosorbent assay (ELISA) kits were used to evaluate the level of serum cardiac troponin-I (cTnI), IL-1β, and IL-18. In addition, the serum lactate dehydrogenase (LDH), and creatine kinase-MB (CK-MB) levels were evaluated *via* an automatic biochemical analyzer (Olympus 5400; Olympus Ltd., Tokyo, Japan).

Myocardial tissue collection and sample processing

After measuring cardiac function, 2 ml of KCl (10%) was injected into the tail vein of the rat to stop the heart activity, followed by removal of the atria and atrial appendages. Then, the heart tissues were cleaned by cold saline. At the midway of the left ventricular long axis, the left ventricle was separated into apical and basal parts parallel to the atrioventricular groove. The apex was introduced to liquid nitrogen, followed by storage at −80°C for quantitative real-time polymerase chain reaction (qRT-PCR) and Western blot analyses. The basal samples were fixed in 4% paraformaldehyde for 12 h, followed by paraffin embedding. The paraffin-embedded samples were sliced into 4-μm sections and then stained with immunohistochemistry (IHC), hematoxylin basic fuchsin-picric acid (HBFP), and hematoxylin and eosin (H&E) staining.

Measurement of myocardial microinfarct size

Early myocardial ischemia or infarct areas were stained with HBFP. Healthy cardiomyocytes' cytoplasm, nuclei, as well as red blood cells (RBCs), and ischemia cardiomyocytes were stained yellow, blue, and red, accordingly. For pathological analysis, the Leica DMR + Q550 system (Leica Microsystem GmbH, Wetzlar, Germany) was employed. The Leica Qwin software was employed to analyze five visual fields from every slice at random. Planimetry was used to determine the area of micro-infarction, represented as a percentage of the overall evaluated region.

Transmission electron microscopy (TEM)

The samples (myocardial tissue) were sliced into 1 mm^3 sections and treated with glutaraldehyde (3%) for 24 h at 4°C. Next, the sections were washed and dried, followed by fixing and staining. These sections were finally examined with using TEM (Hitachi H-7650; Hitachi, Tokyo, Japan).

Immunohistochemistry

The samples (from fresh heart tissue) were paraffinized after being treated with 4% paraformaldehyde. Four-micron sections were taken and deparaffinized, rehydrated, and retrieved with a specific antigen. Endogenous peroxidase activity was inhibited for 25 min at room temperature with a 3% H_2O_2 solution. The sections were treated with 5% bovine serum albumin (BSA) and then incubated (24 h) with primary antibodies including TLR4 (sc-293072, 1:100; Santa Cruz Biotechnology, Dallas, TX, USA), NLRP3 (NBP2-12446, 1:50; Novus Biologicals, Littleton, CO, USA), caspase-1 p20 (sc-398715, 1:100; Santa Cruz Biotechnology), accordingly. The primary antibodies treated sections were exposed (for 50 min) to HRP-linked secondary antibody (1:200, at ~25°C). The sections were counterstained with hematoxylin after being incubated with diaminobenzidine for stain adsorption. A light microscope (Olympus Ltd.) was used to observe the images.

Quantitative real-time PCR

The TRIzol reagent (Invitrogen, Carlsbad, CA, USA) was used for isolating total RNA from cardiac tissues, as suggested by the manufacturer. A NanoDrop2000 spectrophotometer (Thermo Fisher Scientific, Waltham, MA, USA) was employed to determine the concentration as well as purity of RNA. Next, reverse transcription kits (Takara, Kyoto, Japan) were used to synthesize cDNA, followed by their amplification by qRT-PCR *via* SYBR Green I PCR kit (Takara). All qRT-PCR reactions were carried out on the ABI PRISM 7500 system (Applied BioSystems, Foster City, CA, USA). The $2^{-\Delta\Delta Ct}$ technique was evaluated the relative expression of target genes and the internal control was GAPDH. The primer sequences were designed in Table 1.

Western blotting (WB)

A bicinchoninic acid assay kit (P0012S; Beyotime Institute of Biotechnology, Shanghai, China) was used to evaluate the concentration of protein isolated from heart tissues. Sodium dodecyl sulfate polyacrylamide gel electrophoresis (10%–15%) was used for separating a total amount of protein (50 μg) which was then moved onto polyvinylidene difluoride membranes (Millipore, Bedford, MA, USA). Next, non-fat milk was used for membrane blockage at room temperature (for 60 min), followed by incubating at 4°C overnight with primary antibodies: TLR4 (sc-293072, 1:1,000; Santa Cruz Biotechnology), MyD88 (#4283, 1:1,000; Cell Signaling Technology, Boston, MA, USA), p-NF-κB p65 (#3033, 1:1,000; Cell Signaling Technology), NLRP3 (NBP2-12446, 1:1,000; Novus Biologicals), ASC (ab180799, 1:1,000; Abcam, Cambridge, UK), caspase-1 p20 (sc-398715, 1:1,000; Santa Cruz Biotechnology), GSDMD (#39754, 1:1,000; Cell Signaling Technology), IL-1β (sc-12742, 1:1,000; Santa Cruz Biotechnology), IL-18 (ab191860, 1:1,000; Abcam), and GAPDH (ab8245; 1:1,000; Abcam). The membrane washing (five times) was carried out with 1 × TBST buffer solution, followed by incubating with secondary

Table 1. Primers sequences

Genes	Primers sequences (5′-3′)
TLR4	Forward primer (FP): 5′-TATCGGTGGTCAGTGTGCTT-3′
	Reverse primer (RP): 5′-CTCGTTTCTCACCCAGTCCT-3′
NLRP3	FP: 5′-CTCGCATTGGTTCTGAGCTC-3′
	RP: 5′-AGTAAGGCCGGAATTCACCA-3′
IL-1β	FP: 5′-GGGATGATGACGACCTGCTA-3′
	RP: 5′-TGTCGTTGCTTGTCTCTCCT-3′
IL-18	FP: 5′-TGCTCATCATGCTGTTCTGC-3′
	RP: 5′-AGCCAAGAATCTCCGTAGCA-3′
GAPDH	FP: 5′-TTTGAGGGTGCAGCGAACTT-3′
	RP: 5′-ACAGCAACAGGGTGGTGGAC-3′

antibodies conjugated with HRP (ab6721; 1:10,000; Abcam) for 2 h at room temperature. Immunoreactive bands were observed and quantified using an enhanced chemiluminescence kit (Pierce, Rockford, IL, USA), and the ImageJ software (NIH, Bethesda, MD, USA), accordingly.

Statistical analysis

The SPSS version 26 (IBM Co., Armonk, NY, USA) was employed for statistical analyses. The data were represented as mean ± SD. The multiple groups comparison was carried out using the one-way analysis of variance (ANOVA) followed by *post-hoc* test. $p < 0.05$ was statistically significant.

RESULTS

Tanshinone IIA enhanced cardiac function post CME

Relative to the sham group, the cardiac function was considerably lowered in the CME group having low LVFS and LVEF, and high LVESd and LVEDd concentrations. The obtained results of echocardiography were indicated in Fig. 1. Relative to the CME group, Tanshinone IIA pretreatment considerably enhanced cardiac function, as evidenced by raised LVFS and LVEF and lowered LVESd and LVEDd.

Impact of Tanshinone IIA on the myocardial injury markers in serum

As shown in Fig. 2, the obtained data revealed that the levels of cTnI, CK-MB and LDH in the serum of the CME group were considerably elevated than the sham group. In contrast, pretreatment with Tanshinone IIA can dramatically decrease the levels of myocardial damage markers post CME, as indicated by low levels of cTnI, LDH, and CK-MB in the serum of Tan-L and Tan-H groups compared to the CME group.

CME pathological observation

According to H&E and HBFP staining (Fig. 3A, B), the sham group had no apparent myocardial infarction, but subendocardial ischemia was occasionally seen. Multiple microinfarctions were observed in the other three groups, with the majority of them occurring in the subendocardial and left ventricular regions. Furthermore, the nuclei of myocardial cells disintegrated or disappeared in the area of microinfarction triggered by CME, cytoplasmic (red-stained) degenerative changes, peripheral myocardial edema, RBCs exudation, infiltration of peripheral inflammatory cells, and small arterial microembolisms were also observed, according to H&E staining. The myocardial infarct size was considerably decreased in the Tan-L and Tan-H groups, as compared with the CME group, indicating that pretreatment with Tan IIA reduces peripheral myocardial edema and inflammatory cell infiltration, as well as decreases the myocardial infarct size of rats

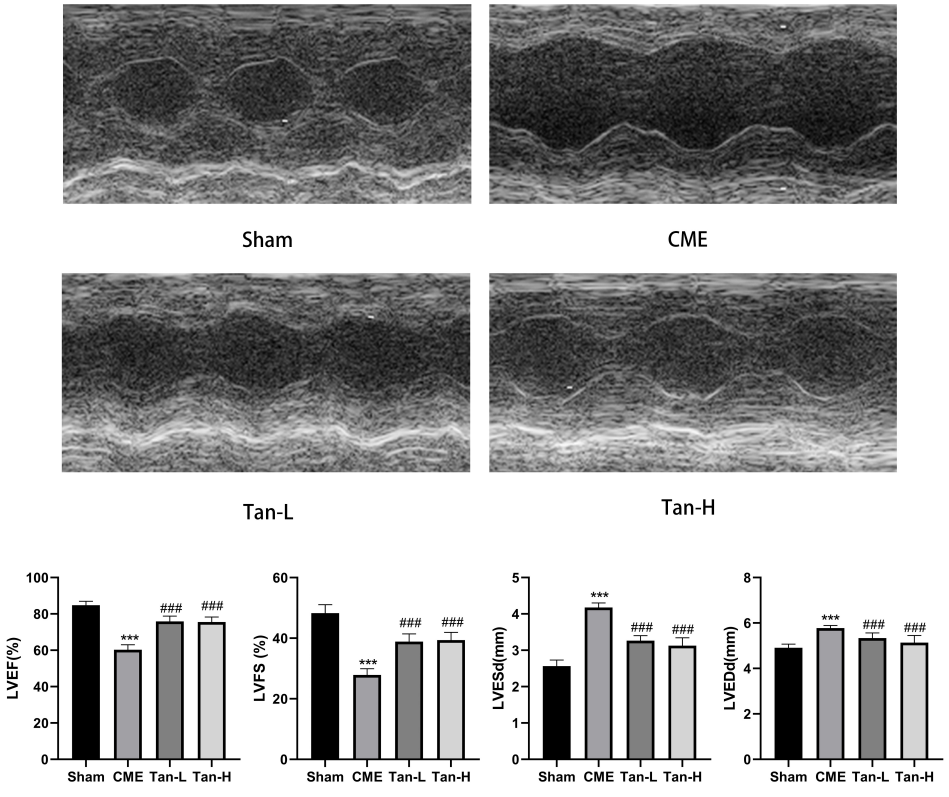

Fig. 1. Echocardiography of rats in each group. The cardiac function parameters of left ventricle ejection fraction (LVEF), left ventricle fractional shortening (LVFS), left ventricular end-diastolic diameter (LVEDd) and left ventricular end-systolic diameter (LVESd) were measured quantitatively (n = 8 per group). The obtained data was revealed as the mean ± SD. CME, coronary microembolization; Tan-L, CME + low-dose Tan IIA (10 mg/kg); Tan-H, CME + high-dose Tan IIA (20 mg/kg). ***$p < 0.001$ *vs.* the sham group; ###$p < 0.001$ *vs.* the CME group.

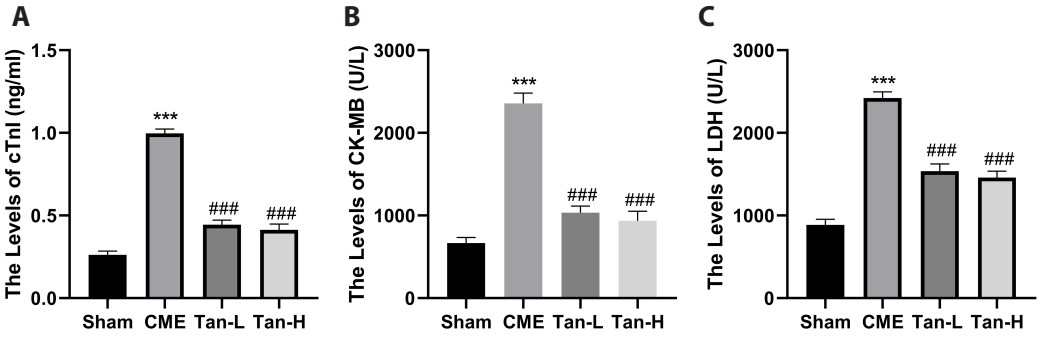

Fig. 2. The serum levels of myocardial injury markers were decreased by Tanshinone IIA (n = 8 per group). The levels of cardiac troponin-I (cTnI), creatine kinase-MB (CK-MB), and lactate dehydrogenase (LDH) in the four groups are indicated in (A–C), respectively. The obtained data was revealed as the mean ± SD. CME, coronary microembolization; Tan-L, CME + low-dose Tan IIA (10 mg/kg); Tan-H, CME + high-dose Tan IIA (20 mg/kg). ***p < 0.001 *vs.* the sham group; ###p < 0.001 *vs.* the CME group.

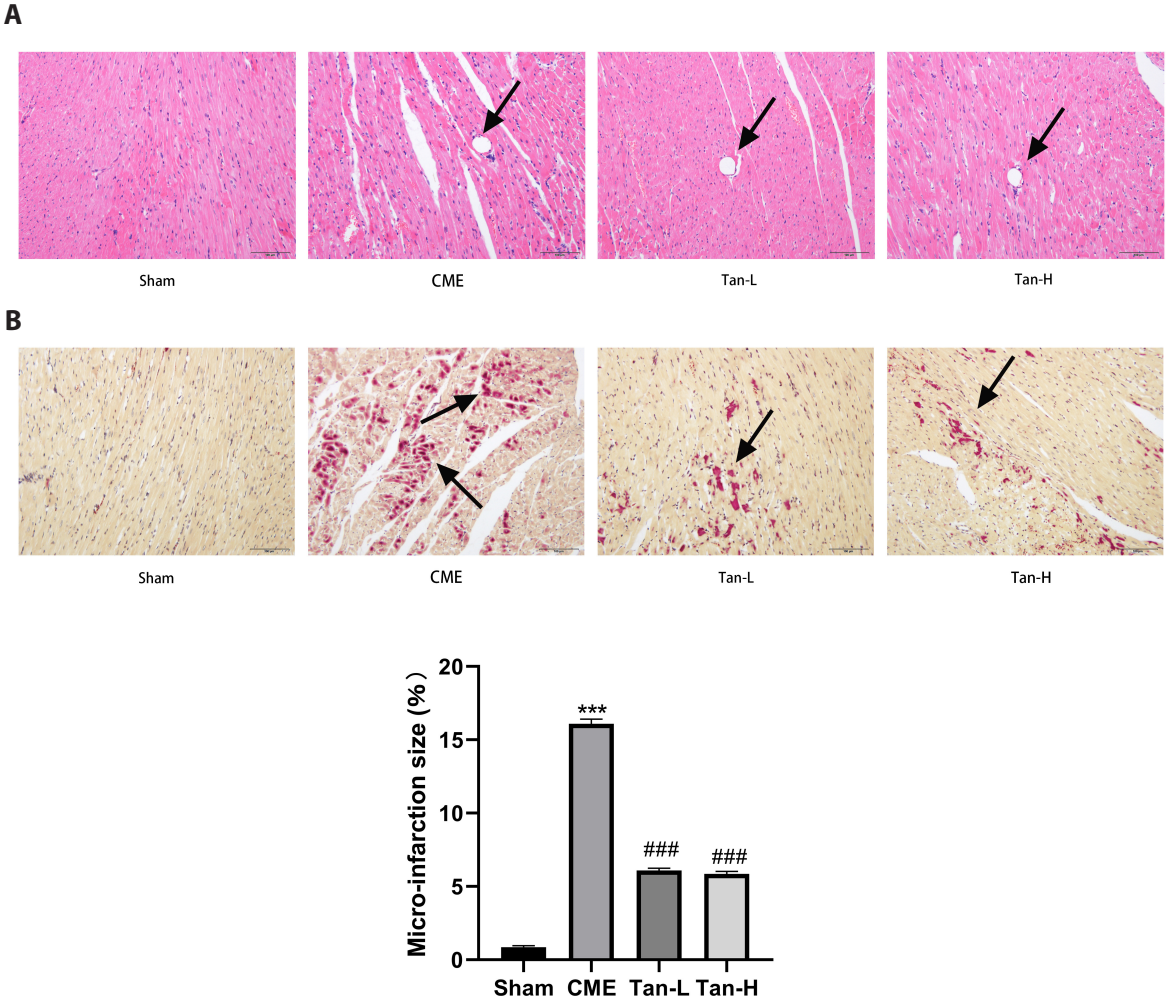

Fig. 3. Histopathological examination of myocardial tissues through hematoxylin and eosin (H&E) and hematoxylin basic fuchsin-picric acid (HBFP) staining (n = 8 for each group). Scale bar = 100 μm. (A) H&E staining. Microspheres with inflammatory cell infiltration were observed in the CME, Tan-L, and Tan-H groups but not in the sham category. The black arrows indicate the microspheres. (B) HBFP staining. An ischemic myocardium is highlighted in red. The black arrows indicate the microinfarct area. CME, coronary microembolization; Tan-L, CME + low-dose Tan IIA (10 mg/kg); Tan-H, CME + high-dose Tan IIA (20 mg/kg). ***p < 0.001 *vs*. the sham group; ###p < 0.001 *vs*. the CME group.

following CME.

Tanshinone IIA may improve CME-induced mitochondrial damage

In the sham group, mitochondria were found to be intact with complete double membranes and crista structures. While in the CME groups, mitochondrial damage was observed including vacuolization, mitochondrial crest rupture, and mitochondrial dysfunction. Minor mitochondrial damage, such as vague cristae and minor vacuolization was found in the Tan-L and Tan-H groups (Fig. 4).

Effect of Tanshinone IIA on cardiomyocyte pyroptosis after CME

To evaluate the impact of Tanshinone IIA on cardiomyocyte pyroptosis after CME, we detected the expression of pyroptosis-related molecules by qRT-PCR, WB, ELISA, and IHC. The results showed that the mRNA levels of IL-1β and IL-18 were considerably elevated in the CME group than in the sham group (Fig. 5A). Meanwhile, the levels of the IL-1β and IL-18 were considerably lowered in the Tan-L and Tan-H group than the CME group.

Western blot analysis was performed to detect the expression of GSDMD-N, caspase-1 p20, IL-18, and IL-1β. Relative to the sham group, the protein levels of caspase-1 p20, GSDMD-N, IL-18, and IL-1β were elevated (Fig. 5B). However, the expression of GSDMD-N, caspase-1 p20, IL-18, and IL-1β was considerably decreased in the Tan-L and Tan-H group than the CME group. The IHC analysis of cardiac tissues (caspase-1 p20), and the serum levels of IL-18, and IL-1β showed consistency with WB results, as indicated in Fig. 5C and D. Taken together, the above results revealed that Tanshinone IIA pretreatment can effectively inhibit cardiomyocyte pyroptosis after CME.

Impact of Tanshinone IIA on the TLR4/MyD88/NF-κB/NLRP3 cascade

The mRNA levels of TLR4 and NLRP3 were considerably elevated in the CME group relative to the sham group, as depicted in Fig. 6A. The levels of TLR4 and NLRP3 were considerably decreased in the Tan-L and Tan-H group than the CME group.

Relative to the sham group, the results of WB showed that the expression of TLR4, MyD88, p-NF-κB p65, NLRP3 and ASC was elevated in the CME group (Fig. 6B). After pretreatment with Tanshinone IIA, the protein levels of TLR4, MyD88, p-NF-κB p65, NLRP3, and ASC were considerably decreased than the CME group. The IHC analysis of cardiac tissues showed consistency with WB results (Fig. 6C). The underlined data suggested that Tan IIA can attenuate cardiomyocyte pyroptosis (CME-induced) potentially through regulation of the TLR4/MyD88/NF-κB/NLRP3 cascade.

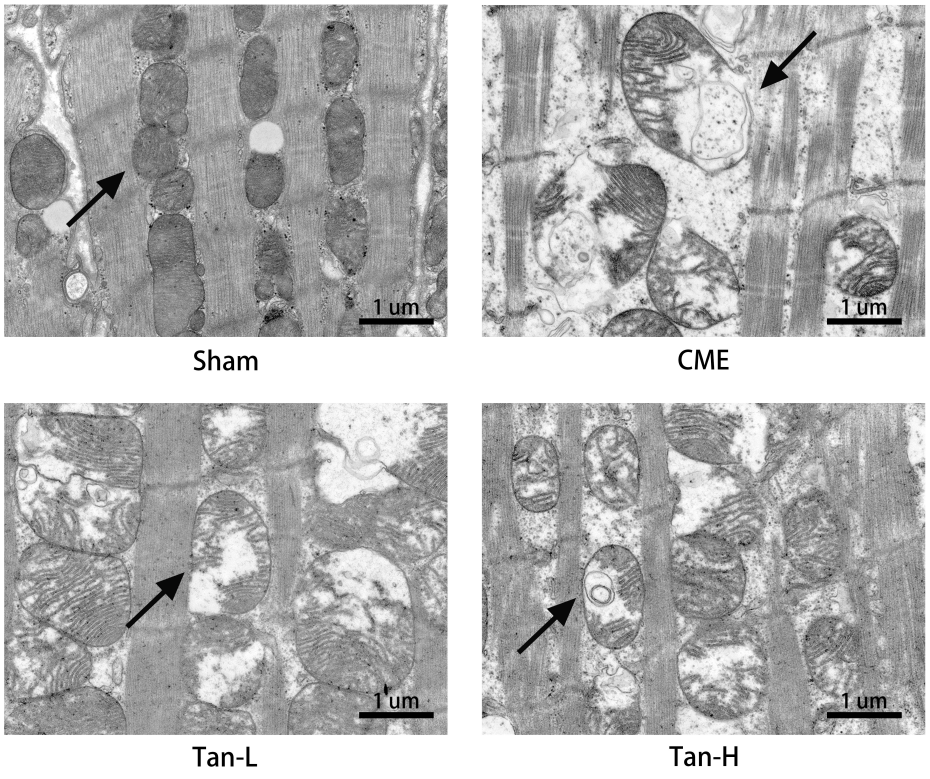

Fig. 4. Myocardial mitochondrial morphology observed by transmission electron microscopy. Scale bar =1 μm. The black arrow represents representative mitochondria. CME, coronary microembolization; Tan-L, CME + low-dose Tan IIA (10 mg/kg); Tan-H, CME + high-dose Tan IIA (20 mg/kg).

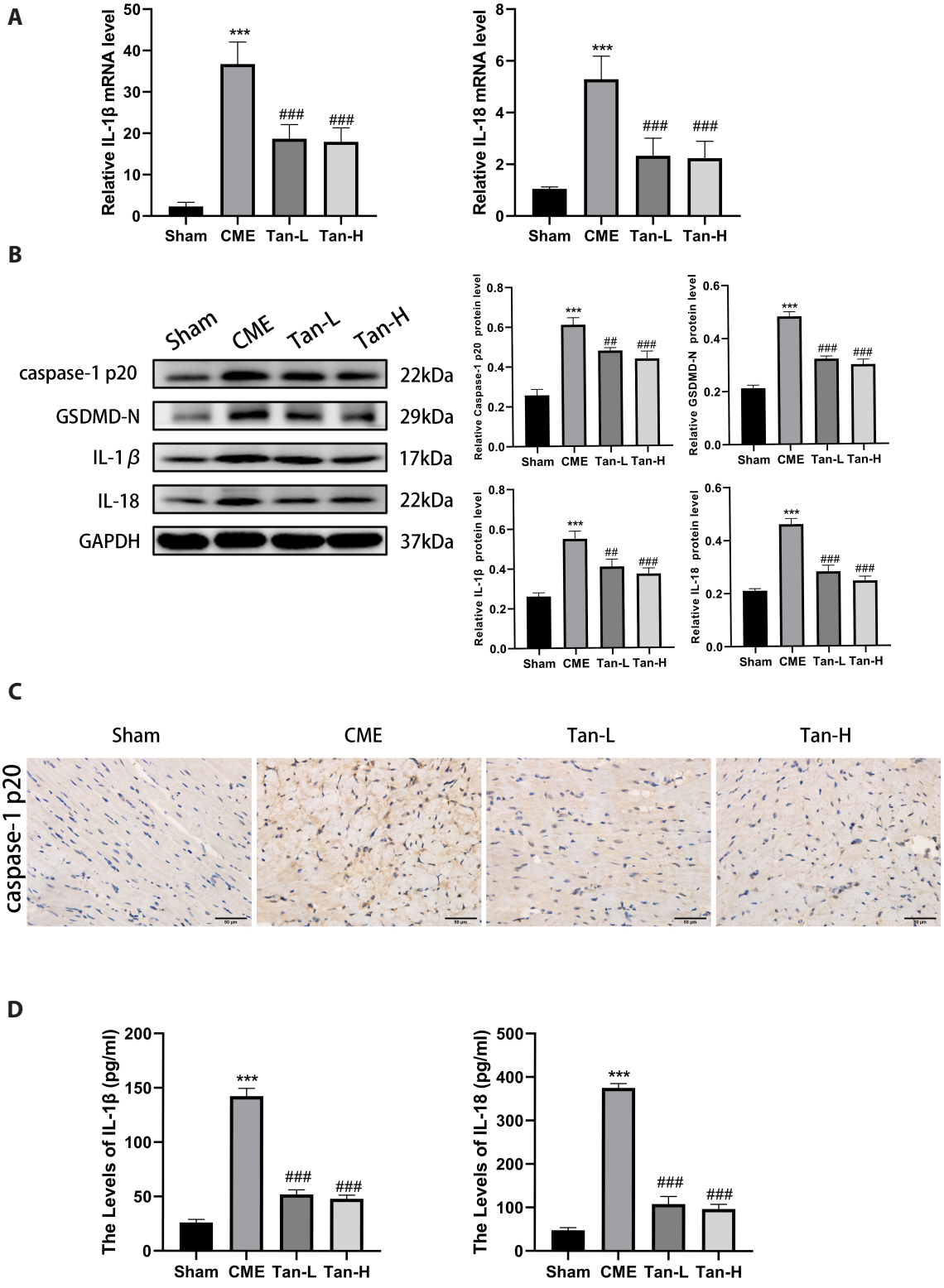

Fig. 5. Tanshinone IIA attenuates cardiomyocyte pyroptosis after CME. (A) The mRNA levels of IL-1β, and IL-18 in the groups (n = 8 for each group). (B) The protein levels caspase-1 p20, GSDMD-N, IL-18, and IL-1β (n = 3 for each group). (C) Representative immunohistochemical pictures of caspase-1 p20 in cardiac tissues. Scale bar = 50 μm. (D) The serum levels of IL-1β and IL-18 markers (n = 8 for each group). The obtained data was revealed as the mean ± SD. CME, coronary microembolization; Tan-L, CME + low-dose Tan IIA (10 mg/kg); Tan-H, CME + high-dose Tan IIA (20 mg/kg). ***p < 0.001 *vs.* the sham group; ##p < 0.01, ###p < 0.001 *vs.* the CME group.

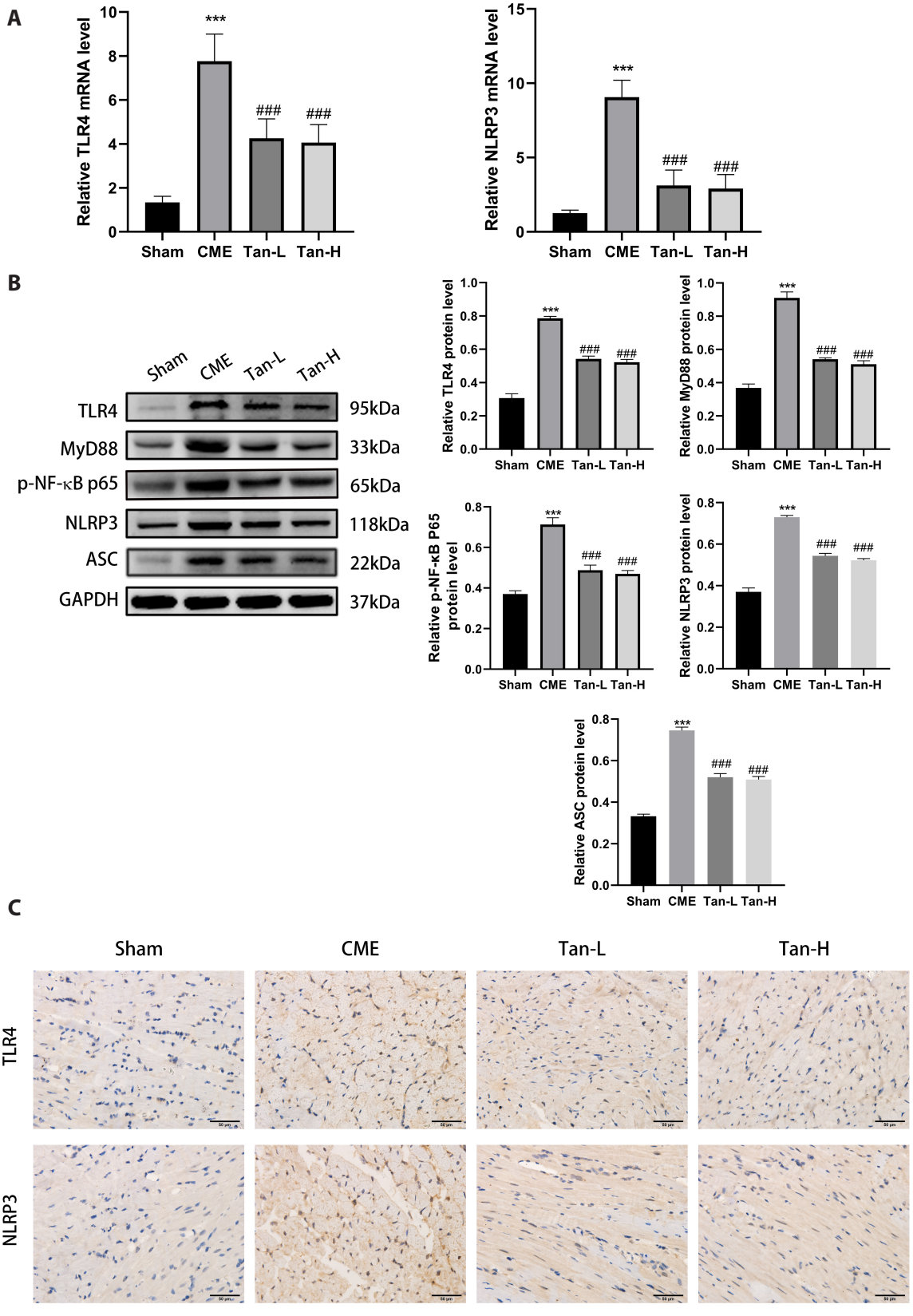

Fig. 6. The inhibition of TLR4/MyD88/NF-κB/NLRP3 cascade by Tanshinone IIA. (A) The mRNA levels of TLR4 and NLRP3 in the groups (n = 8 for each group). (B) The protein levels of TLR4, Myd88, p-NF-κB p65, NLRP3, and ASC (n = 3 for each group). (C) Representative immunohistochemical pictures of TLR4 and NLRP3 in cardiac tissues. Scale bar = 50 μm. The obtained data was revealed as the mean ± SD. CME, coronary microembolization; Tan-L, CME + low-dose Tan IIA (10 mg/kg); Tan-H, CME + high-dose Tan IIA (20 mg/kg). ***p < 0.001 *vs.* the sham group; ###p < 0.001 *vs.* the CME group.

DISCUSSION

Cardiomyocyte pyroptosis occurred after CME, causing myocardial damage and reduction in heart function, according to this study. However, in the CME rat model, Tanshinone IIA pretreatment seven days before triggering CME substantially prevented cardiomyocyte pyroptosis and reduced cardiac damage. Tanshinone IIA may have protected effects against GSDMD activation by attenuating the TLR4/MyD88/NF-κB/NLRP3 cascade, thus reducing the release of pro-inflammatory cytokines IL-1β and IL-18. The impact of Tanshinone IIA on cardiomyocyte pyroptosis in CME rats has never been studied before. These findings showed that Tanshinone IIA pretreatment may provide significant outcomes in the treatment of CME-induced myocardial damage.

Unlike proximal epicardial vascular occlusion, the coronary blood flow is temporarily reduced after CME, but normal perfusion can be restored in a short time, but the cardiac function gradually declines, showing a phenomenon of mismatch between myocardial perfusion and systolic function, which indicates that left ventricular dysfunction induced by CME has not been considerably linked to the decrease of coronary blood perfusion [18]. The current studies revealed that the inflammatory response and apoptotic process of the cardiomyocytes around microinfarction are linked to myocardial damage and progressive cardiac insufficiency post CME. Hence, attenuating myocardial inflammation and apoptotic process of the cardiomyocytes can considerably improve cardiac failure and decrease myocardial injury [19,20]. In the current study, the level of myocardial injury markers elevated, the heart function deteriorated, and myocardial microinfarction appeared in rats after CME. The mitochondria of CME rats' myocardium were swollen and fractured, and the mitochondrial cristae were dissolved, according to TEM. The given results showed consistency with the pathophysiological variations of CME, suggesting the effective CME modeling in rats.

NLRP3 triggers pro-caspase-1 by developing a complex with ASC, IL-1β and IL-18 precursors can be converted into mature inflammatory cytokines when caspase-1 is stimulated. GSDMD is activated after being cleaved by activated caspase 1 to generate GSDMD-N, then transferred to the plasma membrane to form a 10–14 nm transmembrane pore, thereby releasing IL-18, IL-1β, resulting in pyroptosis [21,22]. Pyroptosis has been linked with cardiovascular diseases. Herein, the expression of pro-inflammatory cytokines IL-18, IL-1β, and pyroptosis-associated proteins (caspase-1 p20, GSDMD-N) was considerably elevated in the myocardium post CME, and the underlined results showed consistency with the earlier research.

TLRs are widely distributed, which can directly recognize the highly conserved specific molecular structure shared by certain pathogens or their products, and trigger a series of signal transductions [23,24]. TLR4 is a key upstream immune response regulatory factor. TLR4 activation is linked to NF-κB activation, which regulates proinflammatory cytokine expression [25]. NF-κB is inactive in combination with the inhibitory factor IκB. When the Myd88-dependent signal pathway is activated, Myd88 can activate IκB kinase, allowing IκB phosphorylation and degradation, and then NF-κB is activated and transferred into the nucleus [26], then initiatedthe transcription and expression of NLRP3 and pro-IL-1β. Subsequently, PAMPs or damage/danger-associated molecular patterns induce the activation of NLRP3 inflammasomes, thereby triggering a series of inflammatory cascades. Studies have shown that Sal B and Luteolin can reduce ischemia/reperfusion damage by attenuating the TLR4/NF-κB cascade and NLRP3 inflammasome [27,28]. This study suggested that the levels of MyD88, TLR4, NLRP3, p-NF-κB p65, and ASC expression were considerably elevated post-CME, which indicated the contribution of TLR4/MyD88/NF-κB/NLRP3 cascade in the cardiomyocyte pyroptosis.

Tanshinone IIA can effectively treat cardiovascular diseases, such as myocarditis [29]. However, the impact of the Tanshinone IIA on myocardial damage (CME-induced) is not fully understood. The reported studies have been revealed that Tanshinone IIA contributed to regulating AMPKs/mTOR [30], PI3K/Akt/FOXO3A/Bim [31], MAPK [32], and other classical signaling pathways to reduce myocardial injury. Currently, the relationship between Tanshinone IIA and pyroptosis has not been reported. However, the essence of pyroptosis is also inflammatory death, Tanshinone IIA may inhibit pyroptosis. Herein, Tanshinone IIA pretreatment improved myocardial damage post CME, decreased microinfarct area, and enhanced myocardial function through attenuating cardiomyocyte pyroptosis (CME-induced). Also, we found that Tanshinone IIA significantly attenuated the expression of MyD88, TLR4, p-NF-κB p65, NLRP3, and ASC. Based on the findings, we hypothesized that Tanshinone IIA protects cardiomyocytes from pyroptosis (CME-induced) potentially by blocking TLR4/MyD88/NF-κB/NLRP3 cascade activation, hence lowering myocardial damage.

There are a few limitations to the research. We injected plastic microspheres into the left ventricle of a rat to generate a CME model. Plastic microspheres cannot completely simulate microembolization in clinical patients since it contains platelets, leukocytes, red cells, and atheromatous plaque components. Secondly, it cannot be excluded that atypical cascades of pyroptosis are involved. In addition to the classical pathway dependent on caspase-1, there are also non-classical pathways that depend on caspase-4/5/11, as well as the recently discovered cascade of pyroptosis triggered by caspase-8 [33]. Thirdly, we only evaluated the cardiac function 12 h post CME, and the long-term impact of Tanshinone IIA on CME-induced myocardial damage was not evaluated. Fourthly, we have not evaluated the efficacy of Tanshinone IIA after it was given after the onset of CME. Furthermore, we only studied the effect of different doses of Tanshinone IIA in CME-induced cardiomyocyte pyroptosis, but whether TLR4 activator or inhibitor can reverse or enhance the inhibitory effect

is still unknown. These require further research.

Taken together, the current study revealed that Tanshinone IIA can improve CME-induced cardiomyocyte pyroptosis and enhance cardiac function. The underlying mechanism may involve the TLR4/ MyD88/NF-κB/NLRP3 cascade. Hence, Tanshinone IIA may be useful in the treatment of CME-induced myocardial damage.

FUNDING

This study was supported by the National Natural Science Foundation of China (Grant No.81770346) and the Project for Innovative Research Team in Guangxi Natural Science Foundation (Grant No.2018GXNSFGA281006).

ACKNOWLEDGEMENTS

None.

CONFLICTS OF INTEREST

The authors declare no conflicts of interest.

REFERENCES

1. Bahrmann P, Werner GS, Heusch G, Ferrari M, Poerner TC, Voss A, Figulla HR. Detection of coronary microembolization by Doppler ultrasound in patients with stable angina pectoris undergoing elective percutaneous coronary interventions. *Circulation.* 2007;115:600-608.
2. Heusch G, Kleinbongard P, Böse D, Levkau B, Haude M, Schulz R, Erbel R. Coronary microembolization: from bedside to bench and back to bedside. *Circulation.* 2009;120:1822-1836.
3. Otto S, Seeber M, Fujita B, Kretzschmar D, Ferrari M, Goebel B, Figulla HR, Poerner TC. Microembolization and myonecrosis during elective percutaneous coronary interventions in diabetic patients: an intracoronary Doppler ultrasound study with 2-year clinical follow-up. *Basic Res Cardiol.* 2012;107:289.
4. Heusch G, Skyschally A, Kleinbongard P. Coronary microembolization and microvascular dysfunction. *Int J Cardiol.* 2018;258:17-23.
5. Brennan MA, Cookson BT. Salmonella induces macrophage death by caspase-1-dependent necrosis. *Mol Microbiol.* 2000;38:31-40.
6. Mouasni S, Gonzalez V, Schmitt A, Bennana E, Guillonneau F, Mistou S, Avouac J, Ea HK, Devauchelle V, Gottenberg JE, Chiocchia G, Tourneur L. The classical NLRP3 inflammasome controls FADD unconventional secretion through microvesicle shedding. *Cell Death Dis.* 2019;10:190.
7. Ding J, Wang K, Liu W, She Y, Sun Q, Shi J, Sun H, Wang DC, Shao F. Pore-forming activity and structural autoinhibition of the gasdermin family. *Nature.* 2016;535:111-116. Erratum in: *Nature.* 2016;540:150.
8. Shi J, Zhao Y, Wang K, Shi X, Wang Y, Huang H, Zhuang Y, Cai T, Wang F, Shao F. Cleavage of GSDMD by inflammatory caspases determines pyroptotic cell death. *Nature.* 2015;526:660-665.
9. Takeuchi O, Akira S. Pattern recognition receptors and inflammation. *Cell.* 2010;140:805-820.
10. Han Y, Liao X, Gao Z, Yang S, Chen C, Liu Y, Wang WE, Wu G, Chen X, Jose PA, Zhang Y, Zeng C. Cardiac troponin I exacerbates myocardial ischaemia/reperfusion injury by inducing the adhesion of monocytes to vascular endothelial cells via a TLR4/NF-κB-dependent pathway. *Clin Sci (Lond).* 2016;130:2279-2293.
11. Wang Q, Lin P, Li P, Feng L, Ren Q, Xie X, Xu J. Ghrelin protects the heart against ischemia/reperfusion injury via inhibition of TLR4/NLRP3 inflammasome pathway. *Life Sci.* 2017;186:50-58.
12. Su Q, Li L, Sun Y, Yang H, Ye Z, Zhao J. Effects of the TLR4/Myd88/NF-κB signaling pathway on NLRP3 inflammasome in coronary microembolization-induced myocardial injury. *Cell Physiol Biochem.* 2018;47:1497-1508.
13. Gu Y, Liang Z, Wang H, Jin J, Zhang S, Xue S, Chen J, He H, Duan K, Wang J, Chang X, Qiu C. Tanshinone IIA protects H9c2 cells from oxidative stress-induced cell death via microRNA-133 upregulation and Akt activation. *Exp Ther Med.* 2016;12:1147-1152.
14. Cheng TO. Cardiovascular effects of Danshen. *Int J Cardiol.* 2007;121:9-22.
15. Li Q, Shen L, Wang Z, Jiang HP, Liu LX. Tanshinone IIA protects against myocardial ischemia reperfusion injury by activating the PI3K/Akt/mTOR signaling pathway. *Biomed Pharmacother.* 2016;84:106-114.
16. Li L, Li DH, Qu N, Wen WM, Huang WQ. The role of ERK1/2 signaling pathway in coronary microembolization-induced rat myocardial inflammation and injury. *Cardiology.* 2010;117:207-215.
17. Su Q, Lv X, Sun Y, Ye Z, Kong B, Qin Z. Role of TLR4/MyD88/NF-κB signaling pathway in coronary microembolization-induced myocardial injury prevented and treated with nicorandil. *Biomed Pharmacother.* 2018;106:776-784.
18. Dörge H, Neumann T, Behrends M, Skyschally A, Schulz R, Kasper C, Erbel R, Heusch G. Perfusion-contraction mismatch with coronary microvascular obstruction: role of inflammation. *Am J Physiol Heart Circ Physiol.* 2000;279:H2587-H2592.
19. Liu T, Zhou Y, Wang JY, Su Q, Tang ZL, Liu YC, Li L. Coronary microembolization induces cardiomyocyte apoptosis in swine by activating the LOX-1-dependent mitochondrial pathway and caspase-8-dependent pathway. *J Cardiovasc Pharmacol Ther.* 2016;21:209-218.
20. Wang JY, Chen H, Su X, Zhou Y, Li L. Atorvastatin pretreatment inhibits myocardial inflammation and apoptosis in swine after coronary microembolization. *J Cardiovasc Pharmacol Ther.* 2017;22:189-195.
21. Bergsbaken T, Fink SL, Cookson BT. Pyroptosis: host cell death and inflammation. *Nat Rev Microbiol.* 2009;7:99-109.
22. Liu X, Zhang Z, Ruan J, Pan Y, Magupalli VG, Wu H, Lieberman J. Inflammasome-activated gasdermin D causes pyroptosis by forming membrane pores. *Nature.* 2016;535:153-158.
23. Li H, Wang X, Xu A. Effect of paclitaxel+hirudin on the TLR4-MyD88 signaling pathway during inflammatory activation of human coronary artery smooth muscle cells and mechanistic analysis. *Cell Physiol Biochem.* 2018;50:1301-1317.

24. Michaeli A, Mezan S, Kühbacher A, Finkelmeier D, Elias M, Zatsepin M, Reed SG, Duthie MS, Rupp S, Lerner I, Burger-Kentischer A. Computationally designed bispecific MD2/CD14 binding peptides show TLR4 agonist activity. *J Immunol.* 2018;201:3383-3391.
25. Jiang Q, Yi M, Guo Q, Wang C, Wang H, Meng S, Liu C, Fu Y, Ji H, Chen T. Protective effects of polydatin on lipopolysaccharide-induced acute lung injury through TLR4-MyD88-NF-κB pathway. *Int Immunopharmacol.* 2015;29:370-376.
26. Shih RH, Wang CY, Yang CM. NF-kappaB signaling pathways in neurological inflammation: a mini review. *Front Mol Neurosci.* 2015;8:77.
27. Hu Y, Li Q, Pan Y, Xu L. Sal B alleviates myocardial ischemic injury by inhibiting TLR4 and the priming phase of NLRP3 inflammasome. *Molecules.* 2019;24:4416.
28. Zhang X, Du Q, Yang Y, Wang J, Dou S, Liu C, Duan J. The protective effect of Luteolin on myocardial ischemia/reperfusion (I/R) injury through TLR4/NF-κB/NLRP3 inflammasome pathway. *Biomed Pharmacother.* 2017;91:1042-1052.
29. Gao S, Liu Z, Li H, Little PJ, Liu P, Xu S. Cardiovascular actions and therapeutic potential of tanshinone IIA. *Atherosclerosis.* 2012;220:3-10. Erratum in: *Atherosclerosis.* 2012;221:604.
30. Zhang X, Wang Q, Wang X, Chen X, Shao M, Zhang Q, Guo D, Wu Y, Li C, Wang W, Wang Y. Tanshinone IIA protects against heart failure post-myocardial infarction via AMPKs/mTOR-dependent autophagy pathway. *Biomed Pharmacother.* 2019;112:108599.
31. Zhang MQ, Zheng YL, Chen H, Tu JF, Shen Y, Guo JP, Yang XH, Yuan SR, Chen LZ, Chai JJ, Lu JH, Zhai CL. Sodium tanshinone IIA sulfonate protects rat myocardium against ischemia-reperfusion injury via activation of PI3K/Akt/FOXO3A/Bim pathway. *Acta Pharmacol Sin.* 2013;34:1386-1396.
32. Zhang Y, Zhang L, Chu W, Wang B, Zhang J, Zhao M, Li X, Li B, Lu Y, Yang B, Shan H. Tanshinone IIA inhibits miR-1 expression through p38 MAPK signal pathway in post-infarction rat cardiomyocytes. *Cell Physiol Biochem.* 2010;26:991-998.
33. Sarhan J, Liu BC, Muendlein HI, Li P, Nilson R, Tang AY, Rongvaux A, Bunnell SC, Shao F, Green DR, Poltorak A. Caspase-8 induces cleavage of gasdermin D to elicit pyroptosis during *Yersinia* infection. *Proc Natl Acad Sci U S A.* 2018;115:E10888-E10897.